



Investigating the impact of an Al-Si additive on the resistivity of biomass ashes



Lee J. Roberts^{a,b,*}, Patrick E. Mason^a, Jenny M. Jones^a, William F. Gale^{a,c}, Alan Williams^a,
Connie Ellul^d

^a School of Chemical and Process Engineering (SCAPE), University of Leeds, Leeds LS2 9JT, UK

^b Centre for Doctoral Training in Bioenergy, University of Leeds, Leeds LS2 9JT, UK

^c Centre for Integrated Energy Research, University of Leeds, Leeds LS2 9JT, UK

^d EDF Energy, West Burton Power Station, Retford, Nottinghamshire DN22 9BL, UK

ABSTRACT

Ash resistivity is an important factor in the collection efficiency of electrostatic precipitators (ESPs). There is good experience in the industry regarding resistivity of coal fly ash and well-established models for its prediction based on coal ash composition. The same is not true for biomass ash and this paper reports much-needed data for three different biomass types. Coal pulverised fuel ash (PFA), can be used as an aluminosilicate additive to mitigate biomass ash deposition issues. The effects of PFA additive on the resistivity of biomass ashes is also reported here. Biomass ash resistivity is an order of magnitude lower than that of typical coal ashes, and thus re-entrainment of particles in ESPs may become an operational issue, exacerbated by the presence of moisture and sulphur. PFA additive can increase the resistivity, but also leads to higher ash loading. Regression analysis indicates that potassium in biomass ash impacts significantly upon resistivity, contrary to previous studies. Various existing resistivity models were tested for predicting biomass ash resistivity; they produced significant overestimates when compared to experimental results due to omission of potassium as a component of the ash. Modifications to existing models or new models are required to predict resistivity of biomass ashes, and the data reported here will be important for developing such a model.

1. Introduction

As a result of increased scientific understanding of the effects of atmospheric pollution, most industrialised nations have enforced legislation to limit emissions of fly ash particulates; legislation that will become more stringent as time passes. One of the most effective methods to reduce particulate emissions in combustion plants is through the use of electrostatic precipitators (ESPs), since up to 90% of the ash can be carried upstream within the waste gases [1]. Fly ash compositions emitted into the atmosphere by coal-fired power plants mostly consist of Al_2O_3 , SiO_2 and Fe_2O_3 , which can constitute up to 90% of the total mass [2]. Alongside limits on particulates, emissions of greenhouse gases and other harmful emissions are facing increasingly strict regulation, resulting in power generators turning from coal to alternative fuel sources such as biomass, for which design and operational experience is much more limited. Biomass ashes typically contain relatively high concentrations of CaO , K_2O , P_2O_5 and MgO in comparison to coal ash, leading to different physical behaviour. This can

reduce the efficacy of ESP particulate collection, particularly if super-heater temperature is reduced in response to high temperature corrosion [3].

A number of factors serve to influence fly ash collection efficiency, including particle size, shape and surface properties [1], the choice of discharge electrode depending upon fly ash properties [4], and plate spacing [5]. However, the major effect of particle composition upon ESP performance is related to the electrical resistivity of the deposited material. The resistivity of a material is heavily dependent upon the nature of its structure (for instance, the dimensions of the particle and the nature of the crystalline and amorphous structures present), and is typically a strong function of temperature. Maximum fly ash resistivity typically occurs at 140–160 °C, with a decrease above these temperatures resulting from a volume property of the ash [6]. The value of resistivity of a fly ash particle can affect the required exposure time within the electric field of an ESP by up to a factor of four or more [1].

There are differing figures quoted in studies regarding the optimal resistivities for fly ash collection. Figures of 10^6 – $10^{10} \Omega\text{m}$ [1],

* Corresponding author at: Energy Building, School of Chemical and Process Engineering, University of Leeds, Leeds LS2 9JT, UK.
E-mail address: pljr@leeds.ac.uk (L.J. Roberts).

10^6 – $10^9 \Omega\text{m}$ [7] and 10^2 – $5 \times 10^8 \Omega\text{m}$ [8] are all quoted in the literature. Particles with resistivities above effective operating conditions can result in reverse ionisation, where the deposited particles on the surface of the ESP electrodes tend to retain their charge. This can result in the build-up of voltage on the deposit surface, and in severe cases result in positive ions being emitted from the surface. These ions affect both the electric field of the ESP and neutralise any negative charge on arriving particles, in turn affecting ESP efficiency.

Conversely, conductive fly ash particles with resistivities of $< 10^6 \Omega\text{m}$ can lose their charge so quickly that they are repelled back into the gas stream: even though the particle may be charged multiple times, it is possible that the particle can escape the influence of the ESP and leave the plant without being captured [1]. Low- NO_x burners have been increasingly used to reduce emissions from pulverised fuel (P.F.) boilers and this has significant implications for ESP performance. Their use has been found to increase residual carbon content within fly ash to above 5% [9], a result of the lower oxygen stoichiometry in an attempt to reduce thermal NO_x production. For conductive materials such as unburnt carbon or metallic particles, with resistivities below $10^6 \Omega\text{m}$, particles can leave the plant without being captured [1]. Within this optimal resistivity range, ESP collection efficiency is still affected by changes in resistivity, as shown in Fig. 1.

Much of the previous research on ash resistivity has focused upon ash from coal combustion. The transition from coal to biomass combustion has implications for ash resistivity, due to the previously noted differences in the physical and chemical characteristics of the ash. Although the composition of biomass fly ash has been extensively studied, the resulting resistivity of these compositions, and in turn the effect upon ESP performance, is poorly understood [7,10].

In addition to having different electrical properties, biomass ash behaves differently under heating when compared to coal ash, which poses issues with regards to ash deposition in boilers. The increased concentration of alkali metals in biomass ash is a significant factor, particularly in the presence of silica [11–15]. One method to reduce slagging and fouling deposition problems is the use of additives [16], which modify the composition of the resulting deposit, thereby potentially changing the behaviour of the ash under heating. Aluminium silicate based additives are an appealing option, due to a strong ability to convert vapour and liquid phase KCl and KSiO_3 to potassium aluminium silicates [17]. Al-Si based additives have been shown to improve deposition rates, alkali vapour removal and reduce gaseous alkali concentrations. As the addition of the additive will change the composition of the resulting fly ash, the resistivity will also be affected. The purpose of this study is to examine the changes in biomass ash resistivity resulting from the use of a potential aluminium-silicate based additive for deposition control, coal pulverised fuel ash (PFA), along with analysis of the important ash constituents affecting the ash

behaviour. As the coal PFA is a waste product (coal fly ash) immediately available to power stations, its use as an additive is desirable.

The efficacy of coal PFA as an additive in the mitigation of slagging and fouling [16,18,19] and its effect upon biomass combustion characteristics [20] has been the subject of numerous studies, while the mineralogy of coal is well understood [11,21]. One potential concern with utilizing coal fly ash as an additive during biomass combustion is the concentration of trace elements within the fly ash, where up to 80% of elements such as Cd, Sn and Pb within the source coal may accumulate [22], along with high levels of As and Se, which may not otherwise be present in biomass. These elements are likely to volatilize upon exposure to combustion conditions within the boiler. As this study is focused solely on ash resistivity, trace elements are not present in sufficient quantities to affect resistivity. However, increased Ca, K and Mg content as a result of biomass co-firing has been shown to promote the retention of As within the resulting fly ash, for example, potentially offsetting emissions [23]. While the current work is not focused on this aspect, emissions and elemental partitioning of trace metals during biomass co-firing (which will result in similar fly ash concentrations) have been studied previously [24–27].

2. Experimental method

2.1. Ash characterisation

Three samples of solid biomass fuels typically used in large scale pulverised fuel furnaces for power generation were used in this study, along with an additional fly ash from a co-fired power station. These samples were blended with a potential aluminium-silicate based additive, coal pulverised fuel ash (PFA). All materials were sourced from UK power plant operators: ash analyses are given in Table 1. The olive cake ash (OCA) and bagasse ash (BA) were prepared from raw biomass samples, following British Standards method EN 14775:2009 [28], while the white wood ash (WWA), power station fly ash (FA) and coal PFA samples were supplied in ash form. Moisture and carbon analyses were determined using EN 14775:2009 [28] and EN 14774-3:2009 [29]. The ash compositions were determined through ICP ash analysis.

In addition, the particle size distributions of the ash samples were determined using a Malvern 2000E Mastersizer laser diffraction granulometer. Particle diameter is known to have an effect upon ESP collection efficiency [1] due to the charging mechanism. For particles between 0.18 and $0.7 \mu\text{m}$ both field and diffusion mechanisms are important [30], whereas for larger particles charging from ion collision is the dominant mechanism, resulting in a slight reduction in collection efficiency.

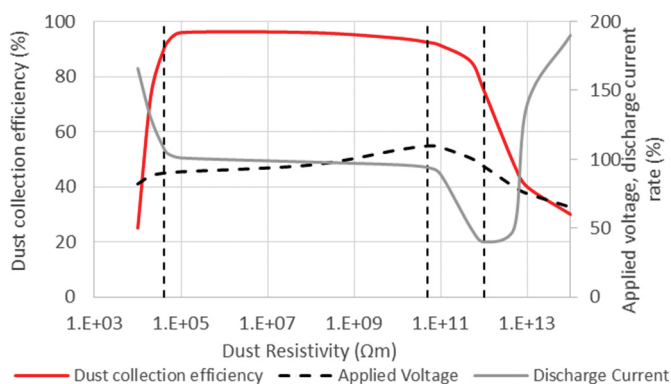


Fig. 1. Collection efficiency vs dust resistivity for electrostatic precipitators. Regions of (from left to right) high re-entrainment, normal operation, excessive sparking and back corona are indicated by the dashed vertical lines. Adapted from [8]

Table 1
Composition of fuels and additive used in this study.

Component	Coal PFA (%)	OCA (%)	WWA (%)	BA (%)	FA (%)
Ash content (wt%)	–	9.87	1.20	4.70	–
Chlorine (d.b)	0.01	0.25	0.01	0.01	–
Sulphur (d.b)	–	0.12	0.02	0.04	–
Moisture in ash (%)	0.48	0.52	0.38	0.26	0.45
Carbon in ash (% d.b)	2.79	1.54	1.43	1.67	1.35
SiO_2	58.2	11.2	27.1	49.7	48.8
Al_2O_3	20.8	1.2	4.6	6.8	19.1
Fe_2O_3	9.3	0.9	2.3	3.0	5.9
CaO	2.9	10.3	24.8	2.9	10.9
MgO	1.4	3.0	4.7	1.5	2.7
Na_2O	2.3	0.6	1.5	0.2	1
K_2O	1.7	32.3	9.2	3.7	6.4
P_2O_5	0.2	5.0	2.0	1.4	0.9
SO_3	0.9	2.4	1.6	0.8	0.6

Table 2
Test matrix of additive-fuel blends used in this study.

% PFA to dry fuel	0%	5%	15%	25%
OCA	X	X	X	X
WWA	X	X	X	X
BA	X	X	X	X
FA	X	X	X	X
PFA	X			

2.2. Ash blending

Alongside the unblended ash samples, three different blend rates of the coal PFA additive with fuel ash samples were studied, at rates equivalent to 5%, 15% and 25% additive to fuel on a wt% basis, as would be used in power generation applications. The ashes were blended at the ratios shown in Table 2, placed into containers and shaken vigorously to produce a homogenous sample. Each sample was again shaken before testing, to maintain homogeneity and to avoid stratification. The calculation to determine the ash content ratio required to simulate a biomass-additive blend is as follows:

$$\frac{\% \text{dry fuel} * \text{dry fuel ash content}}{(\% \text{dry fuel} * \text{dry fuel ash content}) + \% \text{additive}}$$

A test matrix of the ash blends studied are shown below in Table 2.

2.3. Resistivity testing

The ash resistivity testing equipment is based upon the guidelines set out under IEEE standard STD 548-1984 “Standard Criteria and Guidelines for the Laboratory Measurement and Reporting of Fly Ash Resistivity”, as is the methodology used. A schematic of the test cell assembly is shown in Fig. 2. The ash is prepared using the recommended guidelines noted above. The sample is passed through a 177 μm sieve to remove foreign objects. The sample is poured into the test cell until overflowing, at which point a straight-edge is used to strike the ash level with the upper edge of the dish. The dish is agitated to determine if any further settling occurs: if so, additional ash is added and the process repeated. The test cell is placed inside a furnace, to allow for the measurement of ash resistivity over a range of temperatures. The electrodes of the cell are connected to a variable 2 kV power supply, and an ammeter. The furnace door is designed with a magnetic safety-interlock, to isolate the power supply when the door is open.

The resistivity of each ash sample was measured under two sets of conditions, the first with an increasing temperature profile: the samples were heated to 80 °C for approximately 90 min. A voltage was applied to the sample and the current through the sample measured by a high-precision ammeter (Keithley Model 6485). From this, the resistance of

the test sample can be derived. The voltage was increased in steps of 200 V, up to 2 kV. The temperature was then increased to 100 °C, and left for 30 min, before the voltage was again applied. This 30 min period was determined to be the time required for an ash sample to equilibrate with the temperature of the furnace. This was achieved by heating fly ash samples, prepared through the same method as above, in the same furnace and subjected to the same heating rates, with a thermocouple inserted into the sample. This was repeated at 120 °C, 140 °C, 150 °C, 160 °C, 180 °C and 210 °C. The temperatures chosen are different to the standard, where intervals of 30 °C, between 95 °C and 215 °C are recommended. More precise temperature intervals were decided upon, with a particular focus at ESP working temperatures of approximately 150 °C [6]. The resistivity was then calculated from the measured resistance, the fixed cross-sectional area of the test cell and the thickness of the ash sample.

A second set of measurements was made with a decreasing temperature profile. Once a full set of measurements with an increasing temperature profile had been recorded, the sample was heated to 480 °C, as per the standard, and left overnight. The following day, the furnace was switched off and the sample allowed cooling by convection. A voltage was applied to the sample and the current measured at intervals in the same method as previously described, but with a decreasing temperature profile. In accordance with the recommendations of the standard, the results reported are those which produced the highest resistivity value.

In these experiments, the measurements for the decreasing temperature conditions always produced the greatest resistivities. These conditions more accurately simulate those of ash particles within a boiler as they would be moving towards cooler areas, therefore these are the results presented in this study. Measurements were taken at smaller temperature intervals when the sample temperature was around 150 °C, since this is the typical operating temperature of ESPs in coal or biomass fired boilers [6]. Once current measurements were recorded, the resistance at each temperature was calculated for each voltage interval up to 2 kV. From Ohm's law:

$$R = \frac{V}{I}$$

where R is the sample resistance, V is the applied voltage and I is the measured current.

From this, the resistivity, ρ , can be determined, by considering the dimensions of the sample:

$$\rho = \frac{R * A}{d} \quad (1)$$

where d is the depth of ash in the bottom electrode, and A is the surface area of the top electrode.

An important consideration when analyzing the results is that the measured resistivities in this experiment are likely to lead to an over-estimate when compared to the resistivity of the ashes after combustion in a full-scale plant. The most notable difference between experiment and ESP conditions is the lack of water vapour and SO_3 within the samples, which are often present in flue gases of combustion plant, both of which have a significant effect upon the resistivity of the fly ash. The addition of 5% water vapour can reduce resistivity by a factor of 10 at 150 °C, while as little as 1% sulphur reduces resistivity by a factor of 10^4 at 130 °C [1]. The sulphur in the solid fuel burns to produce mostly SO_2 ; however, a small percentage of sulphur produces SO_3 , which can produce sulphuric acid in the presence of moisture. The sulphuric acid condenses below approximately 190 °C upon the surface of the particulates, producing a conductive layer.

In addition, the direct adsorption of SO_3 on particle surfaces may form sulphates, which in turn act as electrolytes [31]. The use of selective catalytic reduction (SCR) for NO_x reduction further promotes the formation of SO_3 from SO_2 and O_2 in the flue gas. Methods to control SO_3 emissions exist, such as the evaporation of anhydrous liquefied

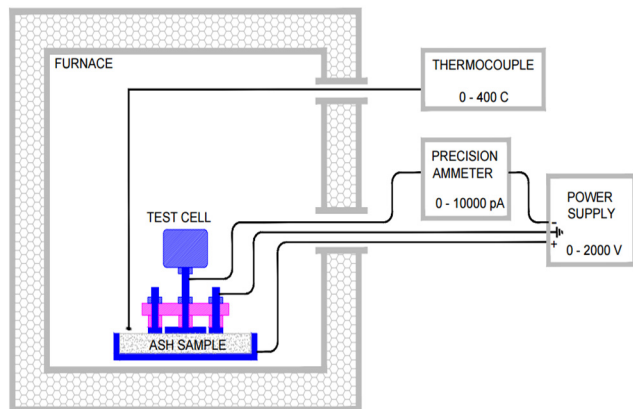


Fig. 2. Schematic of the ash resistivity testing equipment used in this study.

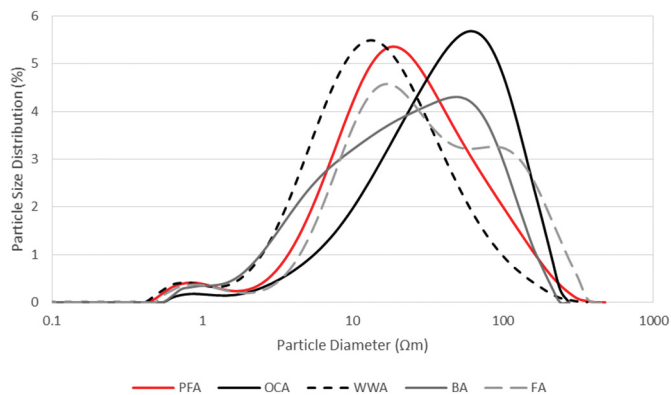


Fig. 3. Particle size distributions for experimental ash samples.

ammonia, which is then mixed with air to produce ammonia injection. The gaseous ammonia then reacts with both SO₃ and SO₂ to produce ammonium sulphate compounds, which serves to increase the cohesivity of the deposit on the collection surface, reducing re-entrainment due to rapping [1].

Nevertheless, the results provide important insight into ash resistivity [32–34], and in this case biomass ash resistivity and how this is influenced by the use of Al-Si additives for deposition control.

3. Results and discussion

3.1. Particle size distributions

Of the samples within this study, the coal PFA and WWA samples contain the highest concentration of submicron particles at 1.5%, while OCA contained the least at 0.6%. The particle size distribution profiles within Fig. 3 are similar to those found in previous studies of biomass fly ashes [35,36]. The greater particle size found within OCA can be attributed to the agglomeration of particles due to the high potassium content. Of note is that the FA sample, which was sourced from a full-scale power station, produced two distinctive peaks. This is in contrast to the coal PFA, which was from a similar source; this difference may be the result of the FA sample being produced from co-firing.

3.2. Resistivity measurements

The ash resistivity measurements presented in Fig. 4a and b show that peak resistivity for OCA/PFA blends and WWA typically occurs at temperatures below 150 °C. Both OCA and WWA have significantly lower resistivities than the coal PFA additive, which was additionally used as a baseline sample. Although the WWA/PFA blends show higher resistivities than PFA, it should be noted that these blends contain > 80% coal PFA concentration; the resistivities are well within the maximum error as outlined by IEEE standard STD 548-1984 (“The results of resistivity determinations carried out by the same mode of measurement (that is, ascending or descending) should not differ by more than a ratio of two (higher/lower)”). The OCA/PFA blends show a clear trend of increasing resistivity with higher additive concentration within the ash at temperatures of above 130 °C. OCA has the lowest

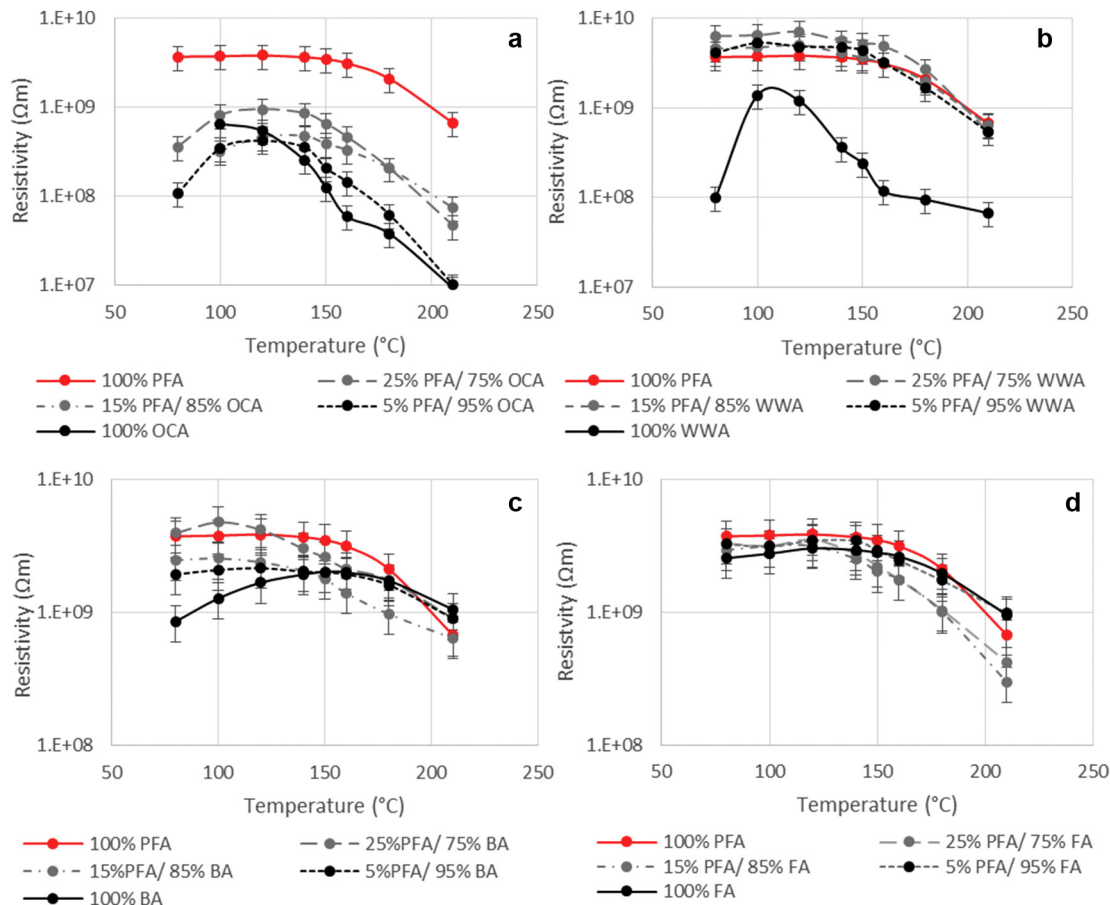


Fig. 4. (a)–(d) Resistivity of (a) olive cake ash (OCA), (b) white wood pellet ash (WWA), (c) bagasse ash (BA), and (d) power station fly ash (FA) blended with a coal PFA additive at different percentages, on a logarithmic scale.

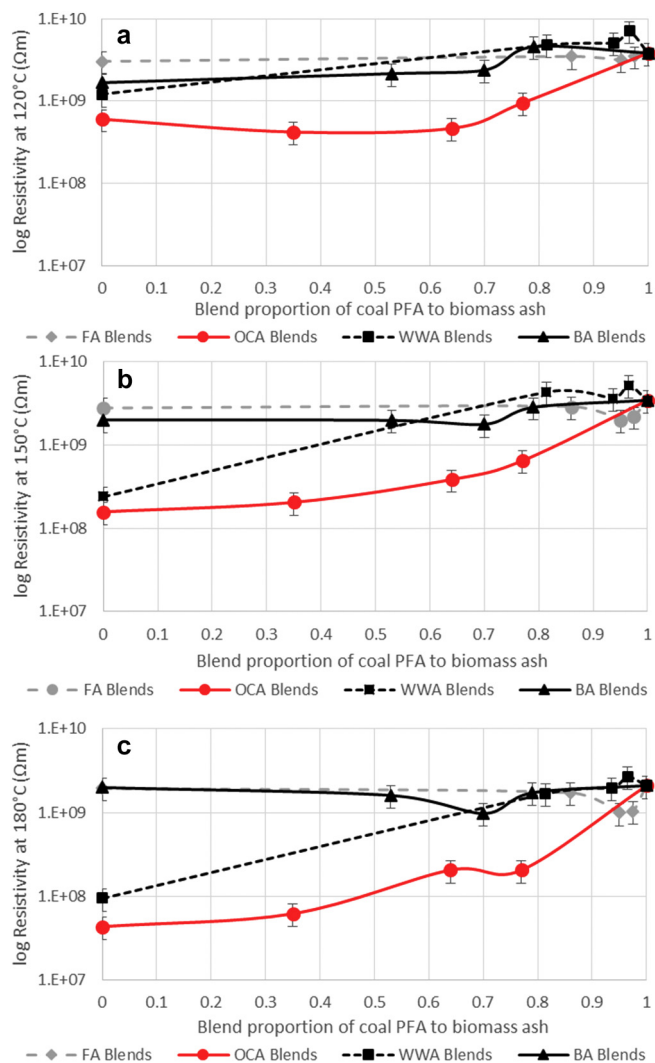


Fig. 5. (a)–(c) Comparison of resistivity results (log scale) at (a) 120 °C, (b) 150 °C and (c) 180 °C with increasing additive concentration.

resistivity of the samples within this study, at $1.58 \times 10^8 \Omega\text{m}$ at 150 °C: in the presence of additional moisture and sulphur from combustion, it is possible that resistivities will be reduced to problematic levels, resulting in poor ESP performance. The use of coal PFA in this case can help to mitigate the issue.

In contrast to OCA and WWA, Fig. 4c and d shows that both BA and FA have significantly higher resistivities, greater by approximately a factor of ~ 10 at 150 °C. Blending coal PFA with FA has the least effect on resistivity out of all of the samples tested, corresponding with the FA having the highest silica and alumina concentration.

Also of note is that, for the biomass ashes, particularly WWA and BA, a decrease in resistivity with decreasing temperature was observed between 150 and 100 °C. This suggests that some surface conductivity effects are present. Previous studies [32–34,37] have reported that Li_2O and Na_2O have a significant reductive effect on both volume and surface resistivity. While the WWA contains 1.0% sodium (atomic concentration), the OCA (0.6%) and particularly the BA (0.2%) samples contain less, suggesting that another factor is responsible. Potassium has been postulated to act as a charge carrier, however multiple studies have found no correlation between potassium and resistivity [32–34,37]. Bickelhaupt found that the migration of potassium ions was present through transference experiments, suggesting that the iron content is crucial in influencing the effect of potassium as a charge carrier, with an increasing iron content promoting additional alkali

metal release in water [38].

These effects provide some explanation for the resistivity profiles in Fig. 4: OCA contains an extremely high concentration of K_2O (32.3%) and little Fe_2O_3 (0.9%), and shows no decrease in resistivity at lower temperatures, implying that surface conductivity effects are negligible. With the addition of coal PFA, which contains an increased iron content (9.3%), a decrease in resistivity is observed in all blended samples at temperatures below 120 °C. In addition, both WWA and particularly BA show signs of surface conductivity at lower temperatures: both samples contain relatively high concentrations of potassium (9.2% and 3.7% respectively), and greater iron content (2.3% and 3.0% respectively) than the OCA. In contrast, the PFA, FA, FA/PFA blends, and WWA/PFA blends (which contain a minimum of 80% coal PFA concentration), no decrease in resistivity with decreasing temperature is observed. This again implies negligible surface conductivity effects. This suggests that the relationship between iron and potassium content is a key factor in affecting resistivity in biomass ash samples. This is discussed further in Section 5.

The resistivity results for each sample and blend tested are compared at normal ESP operating temperatures of 150 °C (Fig. 5b), as defined by Bäck [6]. The OCA and WWA samples, which both contain high alkali metal concentration and low silica compared to the other samples, are affected more by the addition of coal PFA. This effect is magnified at higher temperatures (Fig. 5c). BA, which already has a high silica content, experiences a minimal increase with increasing coal PFA concentration, which at higher temperatures disappears entirely. The FA blends experience little to no change with increasing additive concentration, due to the already high silica and alumina content within the ash.

Although Li et al. and Bickelhaupt report that resistivity is expected to peak at approximately 140–160 °C [32,34], the results for both OCA and WWA in Fig. 5a show an increase in resistivity at 120 °C when compared to Fig. 5b. A significant observation is noted regarding the OCA results at this temperature: in this case, an increase in concentration of coal PFA appears to result in a slight decrease in resistivities, up to a 15% blend or 65% coal PFA concentration. This is possibly due to surface resistivity effects resulting from the presence of sufficient quantities of iron and potassium.

A potential issue when blending fuels with coal PFA, or any additive, is highlighted by the example of OCA. The addition of an additive during biomass firing will serve to increase the total ash content, since it contains little to no carbon. This raises the issue of increased ash loading upon the ESP. While this will also be the case for all biomass-additive blends, the olive cake used in this study already contains a high ash content of 9.87%. Previous operating experience with biomass power plants has seen operational issues occur, where ESP boxes have been reported to be undersized for the purpose of biomass firing [39]. Increasing this further with additives may pose ash loading issues during ESP collection depending on how much of the ash is present in the flue gas. Crucially, however, the coal PFA is expected to convert low melting-point compounds such as potassium silicates and potassium chlorides to potassium aluminium silicates [17], which due to their much higher melting points are less likely to stick to boiler surfaces. This will, in turn, increase the amount of ash passing through the boiler and thereby increase the ash particulate concentration in the flue gases. This may result in a significant effect upon ash loading, in turn reducing collection efficiency.

Additionally, the OCA shows particularly low resistivities that, under real conditions where additional moisture and sulphur is likely to be present, will be close to the lower effective operating limit of ESPs. As the coal PFA additive has a negligible effect upon resistivity at low blend rates, a higher additive concentration would be required to have an effect on resistivity - which may not be feasible. This suggests that olive cake biomass may not be suitable for large scale combustion without some other intervention to increase resistivity, and that although coal PFA has been shown to do so at higher blend rates, this may

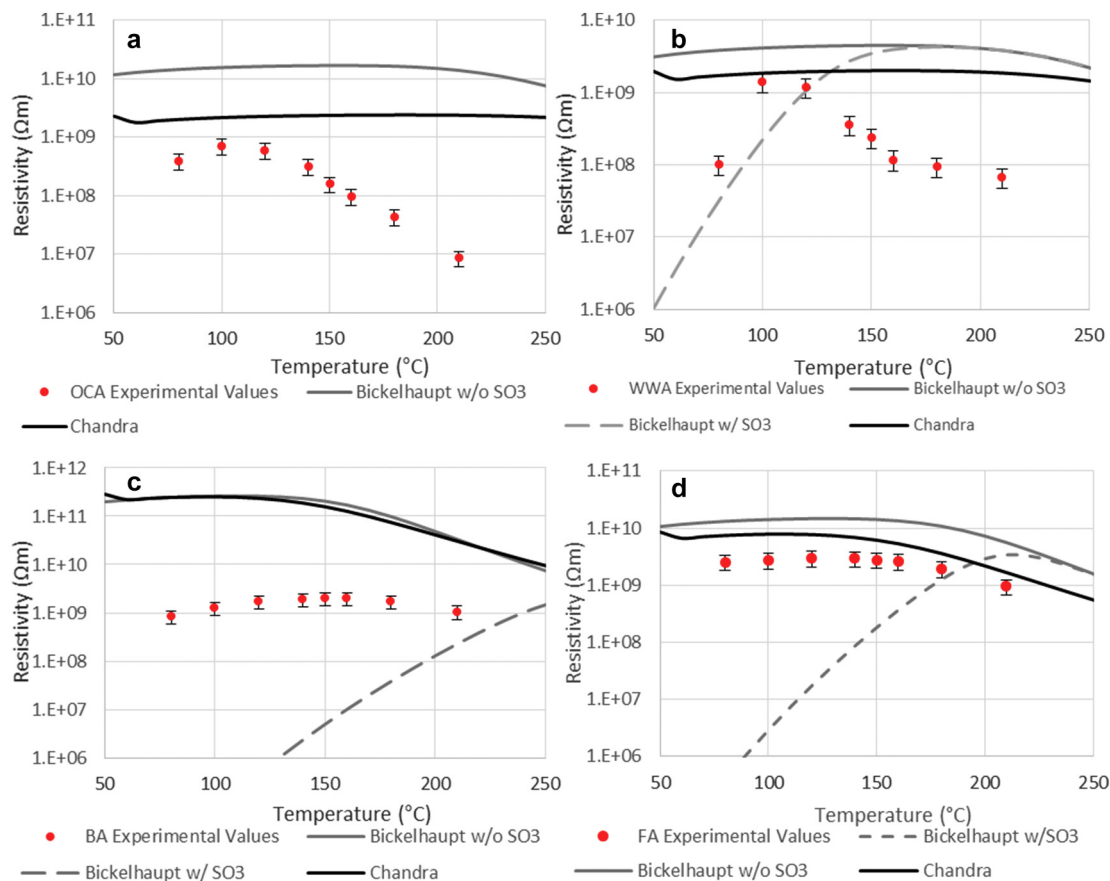


Fig. 6. (a)–(d) Comparison of (a) OCA, (b) WWA, (c) BA and (d) FA experimental resistivities with model predictions. OCA predictions for Bickelhaupt w/SO₃ model gave erroneous results.

Table 3
Comparison of model predictions against maximum recorded resistivity.

Sample	Peak resistivity	Model prediction	Residual	% difference
PFA.	3.83E+09	2.6E+09	1.23E+09	32.10
OCA	7.04E+08	6.84E+08	1.99E+07	2.83
OCA 5%	4.19E+08	4.86E+08	6.70E+07	15.97
OCA15%	4.71E+08	7.24E+08	2.50E+08	53.67
OCA25%	9.48E+08	9.9E+08	4.20E+07	4.40
WWA	1.39E+09	2.26E+09	8.70E+08	62.59
WWA5%	5.29E+09	2.18E+09	3.11E+09	58.75
WWA15%	5.11E+09	2.43E+09	2.68E+09	52.44
WWA25%	7.06E+09	2.5E+09	4.56E+09	64.54
FA	3.01E+09	2.26E+09	7.47E+08	24.83
FA5%	3.46E+09	2.49E+09	9.67E+08	27.95
FA15%	3.12E+09	2.56E+09	5.58E+08	17.88
FA25%	3.48E+09	2.58E+09	9.01E+08	25.88
BA	2.01E+09	5.07E+09	3.10E+09	152.29
BA5%	2.15E+09	3.2E+09	1.00E+09	48.76
BA15%	2.53E+09	2.82E+09	2.90E+08	11.27
BA25%	4.76E+09	2.72E+09	2.05E+09	42.93

only serve to compound the problem.

4. Predictive models and comparison to experimental results

Studies of biomass ash resistivity are scarce [7,10], and as a consequence, no attempts have been made to develop an empirical model for the prediction of biomass ash resistivity. The Bickelhaupt model [32] is often used as a predictive tool for new industrial applications, where an approximation of ash resistivity is necessary in determining ESP size for a specific efficiency [1]. However, as these models are empirically derived from coal ashes, which typically contain 3% or less

potassium within the ash, it is highly likely that the predictions will be invalid for biomass resistivities. The following section is intended to give insight into the mechanisms and important components of resistivity, and to highlight the discrepancy between current available models and biomass compositions.

4.1. Bickelhaupt model

The experimental results were compared to a resistivity model developed by Bickelhaupt [32], originally developed for predicting coal resistivities. The model is made of three components:

- Volume resistivity ρ_v , which is primarily influenced by ash composition
- Surface resistivity ρ_s , which is influenced by both ash composition and water concentration
- Acid resistivity ρ_a , which takes into account the concentration of sulphuric acid in the ash.

In the absence of sulphuric acid, the total resistivity is comprised of the ρ_v and ρ_s components as below.

$$\log \rho_v = -1.8916 \log A_{ls} - 0.9696 \log A_i + 1.237 \log A_{mc} - 0.03E + \frac{4334.515}{T} + 1.5760 \quad (2)$$

$$\log \rho_s = -2.3335 \log A_{ls} - 0.000764 C_w - 0.03E - 0.000321 C_w e^{\left(\frac{2303.3}{T}\right)} + 11.9856 \quad (3)$$

$$\log \rho_a = 25.6528 - 0.3712 C_{SO_3} - \frac{4334.515}{T} - 0.03E \quad (4)$$

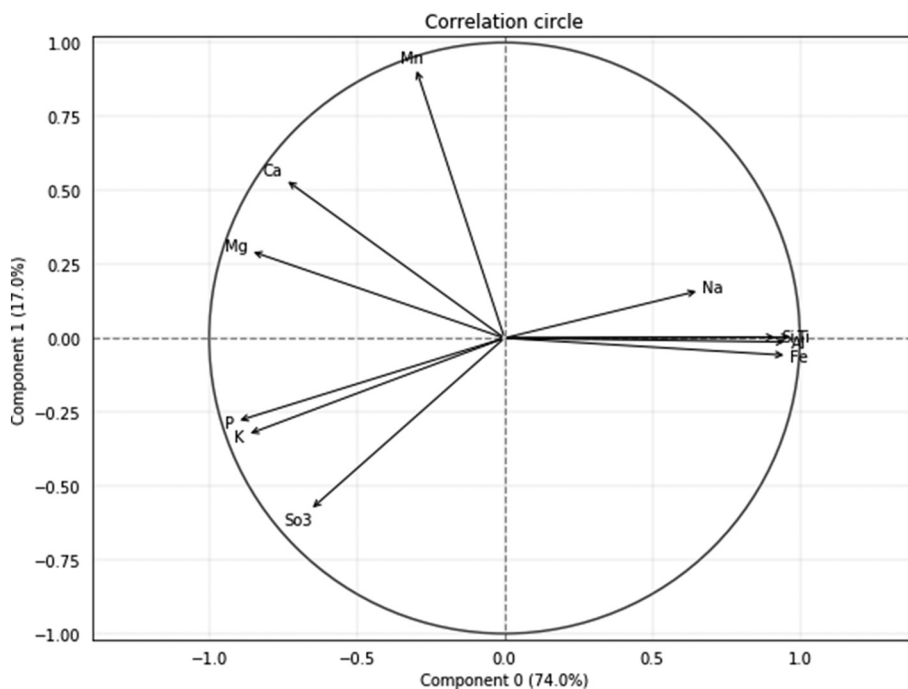


Fig. 7. Correlation circle for ash compositions studied.

Table 4
Correlations between resistivity and atomic concentration of various ash components.

Ash component	Resistivity 120 °C	Resistivity 150 °C	Resistivity 180 °C
Si	0.7243	0.5977	0.5993
Al	0.7184	0.7025	0.7233
Fe	0.7145	0.6981	0.7060
Ca	-0.6273	-0.4250	-0.3729
Ti	0.7441	0.7157	0.7273
Mg	-0.7366	-0.5814	-0.5316
Na	0.3794	0.6548	0.6836
K	-0.9137	-0.8173	-0.7600
Mn	-0.06717	0.1500	0.1881
P	-0.9024	-0.8471	-0.7843
So3	-0.3724	-0.5495	-0.6159
Mg + Ca	-0.6530	-0.4605	-0.4079
K + Fe	-0.8879	-0.7919	-0.7523

$$\frac{1}{\rho_{vs}} = \frac{1}{\rho_v} + \frac{1}{\rho_s} \tag{5}$$

$$\frac{1}{\rho_{vsa}} = \frac{1}{\rho_{vs}} + \frac{1}{\rho_a} \tag{6}$$

where A_{ls} is the atomic concentration of lithium and sodium, A_i is the atomic concentration of iron, and A_{mc} is the atomic concentration of magnesium and calcium. E is electric field intensity in units of kV/cm, T is temperature in K, C_w is water concentration in %, and C_{SO_3} is SO_3 concentration in ppm.

4.2. Chandra modification

A modified version of the model developed by Chandra [33] was also tested. This model is similar but the coefficients are modified and the correction for the effects of SO_3 (Eqs. (2) and (4)) ignored.

$$\log \rho_v = -3.6695 \log A_{ls} - 2.1861 \log A_i + 2.5514 \log A_{mc} - 0.05885E + \frac{3394.117}{T} + 1.4613 \tag{7}$$

$$\log \rho_s = -2.6756 \log A_{ls} - 0.02493C_w - 0.08438E - 0.002169C_w e^{\left(\frac{1870.1284}{T}\right)} + 11.7254 \tag{8}$$

$$\frac{1}{\rho_{vs}} = \frac{1}{\rho_v} + \frac{1}{\rho_s} \tag{9}$$

It is clear from Fig. 6a, b, and c that the models fail to adequately predict the resistivity-temperature relationship of the biomass ashes tested. Nevertheless, the models perform within an acceptable range for the power station fly ash (Fig. 6d): according to IEEE standard STD 548-1984, section 7.4.2, a ratio of 2.7 (higher/lower) is the maximum acceptable variation in resistivity measurements carried out between different laboratories, and as such the models would be expected to perform within this range. As noted above, the Bickelhaupt model (and by extension, the Chandra modification) were developed based upon coal ash studies: as a result, the model is based upon ash compositions containing a maximum of 4.4 wt% K_2O , with the majority of ashes at 3% K_2O or less. As has been established previously, experiments upon biomass ashes and blends have shown that potassium content shows a negative correlation with ash resistivity, although at concentrations of < 3% no visible correlation is present. This indicates that previously developed resistivity models are not representative for biomass ashes such as those investigated in this study, and that with sufficient data, a new predictive model that takes into account high potassium concentration may be produced.

4.3. Maximum resistivity

A third method for modelling resistivity of coal ashes was devised by Li et al. [34]. Rather than focusing upon predicting resistivity over a range of temperatures, the authors determined that only the peak resistivity is of importance, and that it was possible to simplify the problem by only initially considering the lithium + sodium content:

$$\log \rho_{max} = -1.210 \log A_{ls} + \beta \tag{10}$$

where A_{ls} is the combined atomic concentration of lithium and sodium. β is then found by rearranging Eq. (10), and (for an average value of $A_{li} = 0.4$) the normalized resistivity ρ_N determined by:

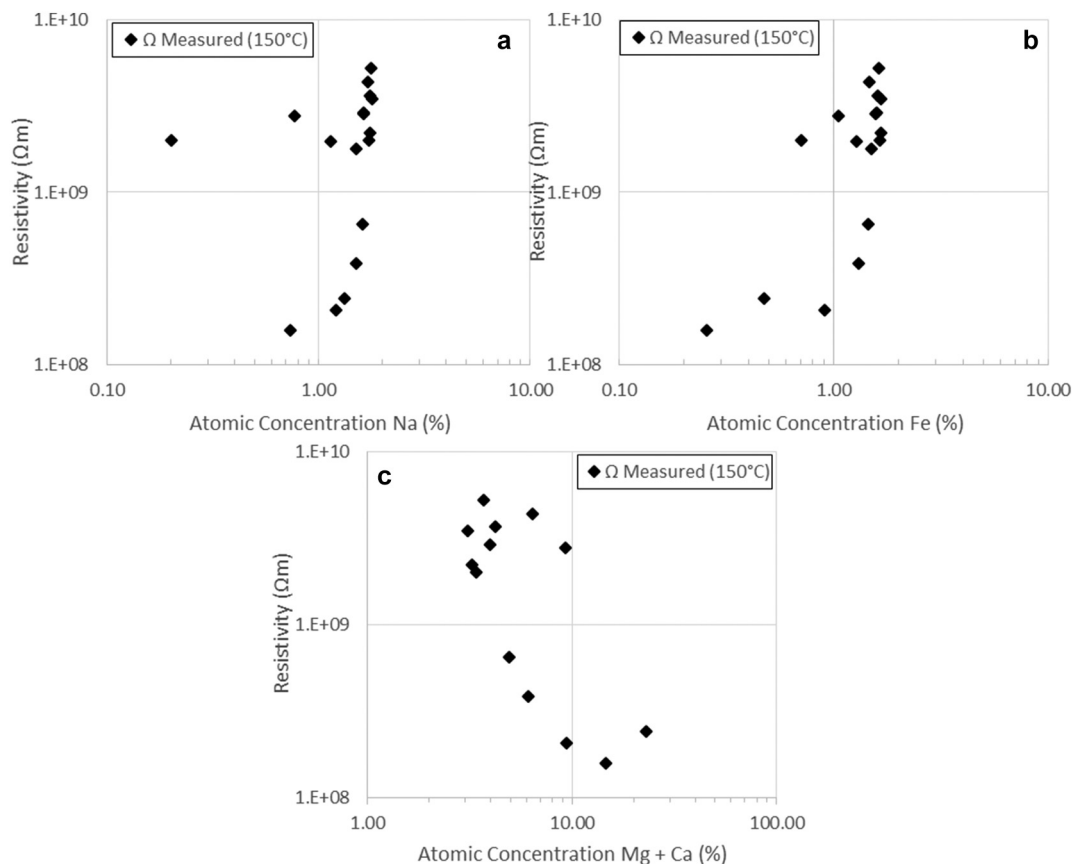


Fig. 8. (a)–(c) Resistivity - concentration relationships at 150 °C for (a) sodium, (b) iron and (c) combined magnesium and calcium concentration.

$$\log \rho_N = \log \rho_{max} + 1.210 \log A_{Is} + 0.48151 \quad (11)$$

As only iron content was found to show a correlation with maximum resistivity, the effect of iron was determined to be:

$$\beta = -0.782 \log A_i + \gamma \quad (12)$$

where γ is related to the water content. When substituted into Eq. (8), this gives the final form of the predictive equation:

$$\log \rho_{max} = -1.210 \log A_{Is} - 0.782 \log A_i + \gamma \quad (13)$$

This equation was applied to the maximum resistivities observed in this study, for all biomass and blends, as shown in Table 3. This model produced accurate predictions for the maximum resistivity of some biomass ash compositions, particularly that of pure OCA, which is particularly surprising given that the model was developed using coal ash compositions and that the OCA contains a significant concentration of potassium. All of the predicted maximum resistivities are well within the 2.7 maximum ratio that is outlined in IEEE standard STD 548-1984. However, in comparison to the Bickelhaupt and Chandra models, this model provides significantly less information: Li et al. created the model with the assumption that maximum resistivity occurs between 140 and 160 °C, while the maximum resistivity of samples within our study range from 100 to 160 °C, outside the operating range of some ESPs. This means that the predicted values are likely to be overestimates of true resistivity at ESP operating temperatures, and in some cases significantly so. In addition, the main effect of potassium is in inducing surface conductivity, which serves to reduce rather than increase resistivity.

5. Composition analysis

5.1. Composition analysis

An analysis of the effect of ash composition upon resistivity was conducted. Previous studies have determined that Mg, Fe, Na, Ca, Al, K and SO₃ content are of primary importance to resistivity values. Principal component analysis (PCA) [40] was conducted upon the composition of the ashes and blends tested in python, in order to determine any correlations between elemental content, as shown in Fig. 7. There is a clear positive correlation between Si and Al content (as expected when increasing alumina-silicate additive concentration). Fe and Ti concentration increase with increasing Si and Al, and a second strong correlation between K and P content exists in the samples and blends studied. Na and K content are shown to be negatively correlated, however the spread of results makes the correlation weak (as indicated by the short length of the Na vector).

5.2. Regression analysis for composition and resistivity

The results were also analysed for correlations at three different recorded temperatures of 120 °C, 150 °C and 180 °C, and regression coefficients are given in Table 4.

Although Ti and P show some of the strongest correlations with resistivity from these results, neither have been shown to have any significant effect upon resistivity in previous studies. Furthermore, the correlation analyses in Fig. 7 show that both correlate with components that are known to affect resistivity (Si, Al and Fe, and K, respectively). Therefore, these components are disregarded. Bickelhaupt recommended that Mg and Ca content should be combined in the model [32]. However, the study on coal showed Mg + Ca to have a positive regression coefficient with resistivity, while the contrary occurs for our

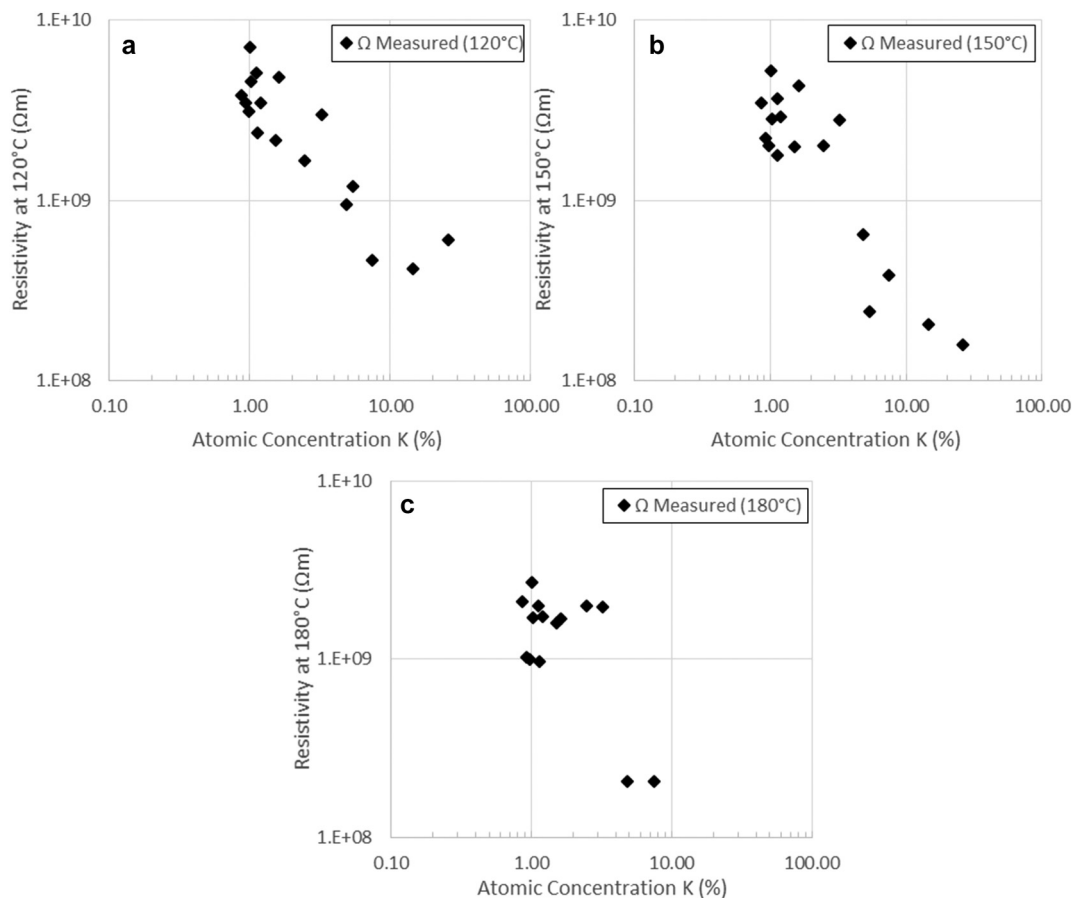


Fig. 9. (a)–(c) Comparison of potassium atomic concentration with resistivity at (a) 120 °C, (b) 150 °C and (c) 180 °C.

data. Additionally, Bickelhaupt suggested that a relationship between potassium and iron content and resistivity exists, whereby the iron content influences the reactivity between the ash and environment, resulting in the release of more potassium ions and thus inducing surface conductivity [37]. The addition of iron content in the analysis does, in this case, result in a strong negative correlation, although this correlation is lower than that of the potassium concentration alone for all temperatures.

Some of the resistivity-component relationships that were described by Bickelhaupt and Li are shown in Fig. 8 for resistivity at 150 °C. Both studies describe a significant negative regression for sodium + lithium content in coal ashes: as lithium is often negligible in biomass ashes, only sodium is considered in this study. Contrary to literature, a positive relationship is found between sodium and resistivity from these experiments (Fig. 8a). This may be the result of sodium having a negative correlation with potassium, coupled with the significantly greater range of potassium concentrations compared to sodium concentrations within this sample set.

This same phenomenon occurs for both iron and Mg + Ca concentration. Iron is described in both Bickelhaupt and Li's study as having the effect of reducing resistivity with increasing concentration, yet the opposite is observed in Fig. 8b. Similarly, Bickelhaupt describes a positive relationship between Mg + Ca concentration and resistivity, while a negative correlation is clearly observed in Fig. 8c.

A notable observation from this study is the relationship between potassium and resistivity: despite both Bickelhaupt and Li finding no correlation of interest, these experiments show a clear developing inverse relationship between potassium content and resistivity at all temperatures measured, shown in Fig. 9 below.

This discrepancy in results between this study and others' is likely related to the concentration of potassium in some of the biomass

samples, which is much greater than those of the coal ashes used in other studies. This can be assessed by conducting linear regression analysis through least squares fitting on the dataset as a whole, and then conducting linear regression on two separate sets of the same data: (i) for less than approximately 3% atomic concentration of potassium, and; (ii) upon the larger levels of potassium concentration. The atomic concentration and resistivity show a non-linear Arrhenius relationship of the form:

$$\rho = e^a * x^b \quad (14)$$

where x is the atomic concentration of the element in the ash, and 'a' and 'b' are determined by least squares fitting. In order to conduct a linear regression, Eq. (14) is given in logarithmic form:

$$\ln \rho = a + b \ln x \quad (15)$$

Doing so reveals that, at temperatures of 120 °C, the negative regression coefficient for all three datasets remains virtually unchanged, indicating that surface resistivity effects may be produced by potassium at all concentrations at this temperature. However, at temperatures of 150 °C and 180 °C, the regression coefficient for samples containing < 3% potassium show virtually no correlation with resistivity, as also reported by Bickelhaupt and Li et al. Higher concentrations of potassium show a clear negative regression coefficient. These regression analyses are presented in Fig. 10.

Applying similar analysis to the relationship between Mg + Ca and resistivity (Fig. 8c) shows a clear difference in behaviour for samples containing > 3% atomic concentration of potassium (Fig. 11). Samples containing < 3% potassium exhibit a similar positive regression coefficient to that reported by Bickelhaupt. This indicates that, at high concentrations, the effect of potassium upon resistivity dominates the effects of other resistivity-affecting components, and must be taken into

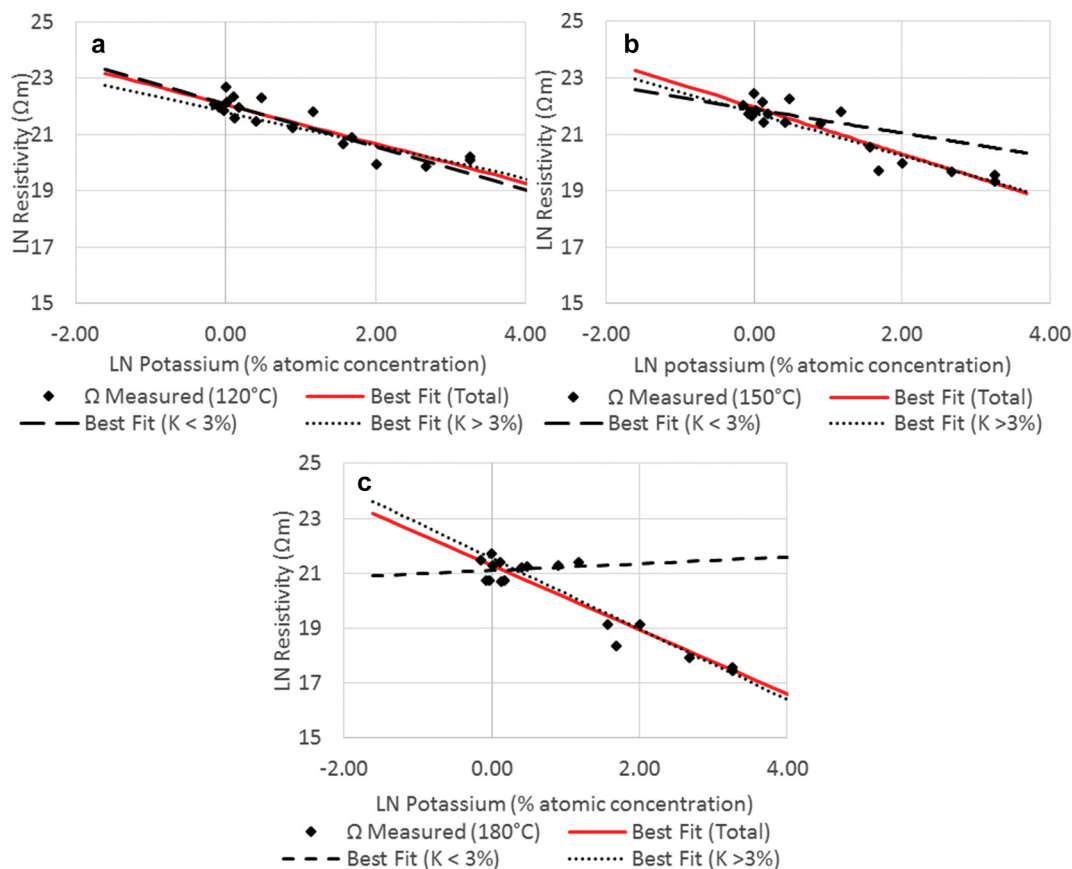


Fig. 10. (a)–(c) Linear regression analysis for resistivity vs potassium concentration at (a) 120 °C, (b) 150 °C and (c) 180 °C.

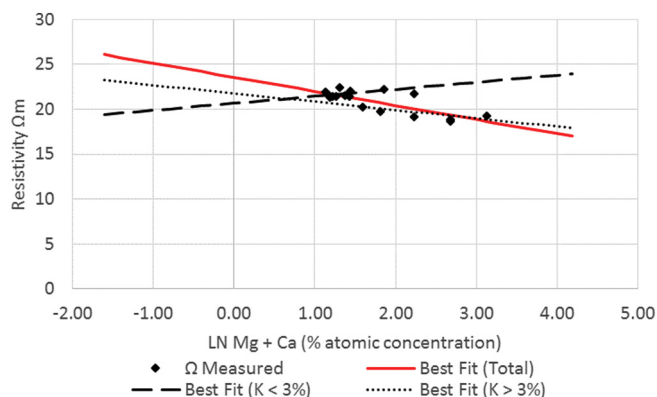


Fig. 11. Linear regression analysis for Mg + Ca concentration with resistivity at 150 °C.

account.

These results imply that, contrary to previous studies, potassium concentration does indeed have an effect upon both the surface and volume resistivity of ash, meaning that while current models may suffice for low potassium levels, at > 3% concentration a previously unknown relationship occurs between potassium and resistivity. As a result, models will need to be modified or developed to describe the resistivity-temperature relationship for such biomass. Additionally, ESP use in biomass firing and co-firing of high potassium biomass will need to be treated significantly differently to when using coal. For instance, the use of sulphur injections to reduce resistivity may be unnecessary for both olive cake and white wood firing, and even for some olive cake blends. In the case of biomass containing high concentrations of potassium (e.g. olive cake), conditioning to increase resistivity may be

required in order to maintain effective resistivities, particularly in the presence of SO₃ and moisture.

6. Conclusions

Aluminosilicate additives have shown promise in improving the deposition characteristics of biomass ashes. However the resulting effects upon resistivity, and in turn ESP performance, are yet to be investigated fully. To determine the resistivity of biomass ashes and biomass-additive blends, a bespoke test assembly has been developed, allowing for the measurement of resistivity over a range of temperatures during both heating and cooling. Three biomass ashes (white wood pellet (WWA), olive cake (OCA) and bagasse (BA)) and a power station fly ash (FA) were used in experiments, along with three different blends of each with an aluminosilicate additive (coal pulverised fuel ash (PFA)) at rates of 5%, 15% and 25% of the total mass of solids into the boiler.

Initial results showed that WWA and OCA had significantly lower resistivities than both the other samples and typical coal ash resistivities, close to lower effective operating limits of ESPs noted in literature. This is likely due to the high potassium content, which is particularly prevalent in OCA and OCA/PFA blends. Full-scale firing would likely include additional SO₃ and moisture, which can significantly reduce resistivity, indicating that caution is needed when using some biomass fuels. In contrast, BA displayed significantly higher resistivities compared to the other biomass, comparable to the power station fly ash and coal PFA additive.

In general, increasing coal PFA concentration during combustion leads to increased resistivities. The addition of coal PFA to WWA significantly increases the resistivity by a factor of 26, even at low blends, due to the low ash content of white wood pellets. BA blends show a small increase with increasing PFA concentration, while the FA blends

show no significant change in resistivity with increasing PFA concentration. OCA blends show a trend of increasing resistivity with increased additive concentration, although at a 5% blend rate this increase is negligible. However, the addition of coal PFA will lead to increased ash loading within ESPs, both due to the additive itself and the formation of higher melting point compounds, resulting in less deposition and greater matter reaching the ESP. This is particularly an issue for olive cake, which already has a high ash content (9.78%).

Composition and linear regression analysis shows that, contrary to previous studies, there is a definite negative correlation between potassium concentration and resistivity, suggesting that potassium has an impact on resistivity over a wide temperature range. Separate linear regression analyses for potassium concentrations of < 3% and > 3% K₂O reveal that, at concentrations of < 3%, a regression coefficient of close to zero is observed at temperatures of 150 °C and 180 °C, corresponding with literature, while a significant negative coefficient is visible at higher concentrations. Applying this method to other elements reveals a change in behaviour at high potassium concentrations, as the effect of the potassium upon resistivity saturates the effects of other ash components. This implies that potassium has a greater effect on particle resistivity than previously assumed, in turn suggesting that biomass must be treated very differently to coal ashes.

The effectiveness of three predictive resistivity models was tested. Both the Bickelhaupt and Chandra models were found to significantly overestimate the resistivity of the biomass samples, due to their omission of the effects of potassium. The Li model showed accuracy in producing the maximum resistivity of both biomass and blend samples, especially OCA, suggesting that the potassium content is not significant in determining the maximum resistivity of the sample. However, the model makes a number of assumptions, including that the maximum resistivity occurs between 140 and 160 °C, whereas the maximum resistivities found within this study range from 100 to 160 °C. In addition, if the peak resistivity does not occur at the desired ESP working temperature, this means that the model will produce an overestimate. As a result, current available models are not suitable for predicting biomass resistivity, and with additional data, a new model may be developed for biomass ash taking into account the effect of potassium: the initial correlations here are the first step in developing such a model.

Acknowledgements

The authors would like to thank the Biomass and Fossil Fuel Research Alliance (BF2RA, Grant number 22), for providing funding and expertise to the project, and for the supply of samples used in this study. L. J. Roberts is grateful to the EPSRC Centre for Doctoral Training in Bioenergy (Grant number: EP/L014912/1) for the award of a postgraduate studentship.

References

- [1] K. Parker, Electrical operation of electrostatic precipitators, Power and Energy Series, vol. 41, Institution of Electrical Engineers, London, 2003.
- [2] A. Jaworek, A. Krupa, T. Czech, Modern electrostatic devices and methods for exhaust gas cleaning: a brief review, J. Electrostat. 65 (3) (2007) 133–155.
- [3] T. Nussbaumer, Combustion and co-combustion of biomass: fundamentals, technologies, and primary measures for emission reduction, Energy Fuel 17 (6) (2003) 1510–1521.
- [4] M. Jedrusik, A. Świerczok, The influence of fly ash physical and chemical properties on electrostatic precipitation process, J. Electrostat. 67 (2–3) (2009) 105–109.
- [5] B. Navarrete, et al., Influence of plate spacing and ash resistivity on the efficiency of electrostatic precipitators, J. Electrostat. 39 (1997) 65–81.
- [6] A. Bäck, Enhancing ESP efficiency for high resistivity fly ash by reducing the flue gas temperature, in: K. Yan (Ed.), Electrostatic Precipitation: 11th International Conference on Electrostatic Precipitation, Hangzhou, 2008, Springer Berlin Heidelberg, Berlin, Heidelberg, 2009, pp. 406–411.
- [7] T. Nussbaumer, Characterisation of particles from wood combustion with respect to health relevance and electrostatic precipitation, 3rd Mid-European Biomass Conference, Austrian Biomass Association, Graz, 2011.
- [8] A. Mizuno, Electrostatic precipitation, IEEE Trans. Dielectr. Electr. Insul. 7 (5) (2000) 615–624.
- [9] J.M. Beér, Combustion technology developments in power generation in response to environmental challenges, Prog. Energy Combust. Sci. 26 (4–6) (2000) 301–327.
- [10] A. Jaworek, et al., Properties of biomass vs. coal fly ashes deposited in electrostatic precipitator, J. Electrostat. 71 (2) (2013) 165–175.
- [11] R.W. Bryers, Fireside slagging, fouling, and high-temperature corrosion of heat-transfer surface due to impurities in steam-raising fuels, Prog. Energy Combust. Sci. 22 (1) (1996) 29–120.
- [12] L.L. Baxter, et al., The behavior of inorganic material in biomass-fired power boilers: field and laboratory experiences, Fuel Process. Technol. 54 (1–3) (1998) 47–78.
- [13] M. Aho, J. Silvennoinen, Preventing chlorine deposition on heat transfer surfaces with aluminium–silicon rich biomass residue and additive, Fuel 83 (10) (2004) 1299–1305.
- [14] M.U. Garba, Prediction of Ash Deposition for Biomass Combustion and Coal/Biomass Co-combustion, Leeds, University of Leeds, 2012.
- [15] X.C. Baxter, et al., Study of Miscanthus x giganteus ash composition – variation with agronomy and assessment method, Fuel 95 (2012) 50–62.
- [16] H. Wu, et al., Impact of coal fly ash addition on ash transformation and deposition in a full-scale wood suspension-firing boiler, Fuel 113 (2013) 632–643.
- [17] Y. Shao, et al., Ash deposition in biomass combustion or co-firing for power/heat generation, Energies 5 (12) (2012) 5171.
- [18] V. Barišić, K. Peltola, E. Coda Zabetta, Role of pulverized coal ash against agglomeration, fouling, and corrosion in circulating fluidized-bed boilers firing challenging biomass, Energy Fuel 27 (10) (2013) 5706–5713.
- [19] L. Wang, et al., A critical review on additives to reduce ash related operation problems in biomass combustion applications, Energy Procedia 20 (2012) 20–29.
- [20] D.S. Clery, et al., The effects of an additive on the release of potassium in biomass combustion, Fuel 214 (2018) 647–655.
- [21] E. Raask, Mineral Impurities in Coal Combustion: Behavior, Problems, and Remedial Measures, Hemisphere Publishing Corporation, 1985.
- [22] P. Danihelka, et al., Emission of trace toxic metals during pulverized fuel combustion of Czech coals, Int. J. Energy Res. 27 (13) (2003) 1181–1203.
- [23] C. Zhou, et al., Combustion characteristics and arsenic retention during co-combustion of agricultural biomass and bituminous coal, Bioresour. Technol. 214 (2016) 218–224.
- [24] M. Izquierdo, et al., Influence of the co-firing on the leaching of trace pollutants from coal fly ash, Fuel 87 (10) (2008) 1958–1966.
- [25] H. Wu, et al., Trace elements in co-combustion of solid recovered fuel and coal, Fuel Process. Technol. 105 (2013) 212–221.
- [26] M.M. Mokhtar, R.M. Taib, M.H. Hassim, Understanding selected trace elements behavior in a coal-fired power plant in Malaysia for assessment of abatement technologies, J. Air Waste Manage. Assoc. 64 (8) (2014) 867–878.
- [27] Z. Gogebakan, N. Selçuk, Trace elements partitioning during co-firing biomass with lignite in a pilot-scale fluidized bed combustor, J. Hazard. Mater. 162 (2) (2009) 1129–1134.
- [28] British Standards Institute, Solid Biofuels - Determination of Ash Content, (2009).
- [29] British Standards Institute, Solid Biofuels - Determination of Moisture Content - Oven Dry Method, (2009).
- [30] B. Jean-Pascal, Nucleation and aerosol processing in atmospheric pressure electrical discharges: powders production, coatings and filtration, J. Phys. D: Appl. Phys. 39 (2) (2006) R19.
- [31] K.B. Schnelle, R.F. Dunn, M.E. Ternes, Air Pollution Control Technology Handbook, Second edition, CRC Press, 2015.
- [32] R. Bickelhaupt, A Technique for Predicting Fly Ash Resistivity, U.S. Environmental Protection Agency, Research Triangle Park, North Carolina, 1979.
- [33] A. Chandra, Some investigations on fly ash resistivity generated in Indian power plants, in: K. Yan (Ed.), Electrostatic Precipitation: 11th International Conference on Electrostatic Precipitation, Hangzhou, 2008, Springer Berlin Heidelberg, Berlin, Heidelberg, 2009, pp. 399–405.
- [34] X. Li, et al., Sensitivity analysis on the maximum ash resistivity in terms of its compositions and gaseous water concentration, J. Electrostat. 70 (1) (2012) 83–90.
- [35] T. Lind, et al., Volatilization of the heavy metals during circulating fluidized bed combustion of forest residue, Environ. Sci. Technol. 33 (3) (1999) 496–502.
- [36] K. Ohenoja, et al., Effect of particle size distribution on the self-hardening property of biomass-peat fly ash from a bubbling fluidized bed combustion, Fuel Process. Technol. 148 (2016) 60–66.
- [37] R.E. Bickelhaupt, Surface resistivity and the chemical composition of fly ash, J. Air Pollut. Control Assess. 25 (2) (1975) 148–152.
- [38] R. Bickelhaupt, Effect of Chemical Composition on Surface Resistivity of Fly Ash, Environmental Protection Agency: National Service Center for Environmental Publications (NSCEP), 1975, p. 51.
- [39] G. Wiltsee, N.R.E. Laboratory, Lessons Learned from Existing Biomass Power Plants, NREL, 2000.
- [40] S. Wold, K. Esbensen, P. Geladi, Principal component analysis, Chemom. Intell. Lab. Syst. 2 (1) (1987) 37–52.